

**TITLE:**

FLOW ANALYSIS AND SEPARATION OF EXFOLIATED  
RESPIRATORY TRACT CELLS

**AUTHOR(S):**

J. A. Steinkamp, K. M. Hansen, J. S. Wilson,  
and G. C. Salzman

**SUBMITTED TO:**

To be presented at the Third International Symposium  
on Pulse Cytophotometry, to be held in Vienna, Austria  
(March 30-April 1, 1977); to be published in the  
Proceedings by European Press, Ghent, Belgium

**NOTICE**  
This report was prepared by an individual who  
operated under a contract with the United States  
Government. The United States Government is authorized  
to reproduce and distribute reprints for Government  
purposes not withstanding any copyright notation  
thereon. This report is the property of the United States  
Government and is loaned to your organization; it and  
its contents are not to be distributed outside your  
organization.

By acceptance of this article for publication, the  
publisher recognizes the Government's (license) rights  
in any copyright and the Government and its authorized  
representatives have unrestricted right to reproduce in  
whole or in part said article under any copyright  
secured by the publisher.

The Los Alamos Scientific Laboratory requests that the  
publisher identify this article as work performed under  
the auspices of the USERDA.

  
**los alamos**  
**scientific laboratory**  
of the University of California  
LOS ALAMOS, NEW MEXICO 87544

An Affirmative Action/Equal Opportunity Employer

REPRODUCTION OF THIS DOCUMENT IS UNRESTRICTED

FLOW ANALYSIS AND SEPARATION OF  
EXFOLIATED RESPIRATORY TRACT CELLS

Running title: Flow Analysis of Respiratory Cells

J. A. Steinkamp, K. M. Hansen, J. S. Wilson, and G. C. Salzman

Biophysics and Instrumentation Group, Los Alamos Scientific Laboratory

University of California, Los Alamos, New Mexico 87545

### ABSTRACT

This paper describes results of preliminary experiments designed to develop automated flow-analysis methods for determining damage to respiratory tract cells in humans exposed by inhalation of physical and chemical toxic agents, the specific goal being the determination of early atypical changes in exposed lung epithelium using the Syrian hamster as a model test system. Hamster respiratory cell samples composed of macrophages, leukocytes, ciliated columnar, and basal undifferentiated cells were obtained by lavaging the lungs with physiological saline. Cell samples stained with fluorescent dyes specific for various biochemical parameters were analyzed in liquid suspension as they flowed through a chamber intersecting a laser beam of exciting light. Sensors measured the fluorescence and light-scatter optical signals on a cell-by-cell basis. Cellular parameters proportional to optical signals (e.g., enzymatic esterase activity, cell size, DNA content, protein, nuclear and cytoplasmic diameter) were displayed as frequency distribution histograms. Cells were also separated electronically and identified microscopically. The basic operating features of the technology are presented, along with representative examples of results which illustrate initial characterization of normal exfoliated respiratory tract cells.

## INTRODUCTION

The application of advanced flow-analysis methods to measure physical and biochemical properties of cells from the respiratory tract provides a new approach for assessing damage to lung epithelium of humans exposed by inhalation of toxic agents (1-3). This includes the development of automated methods for determining early atypical cellular changes in exfoliated respiratory cells from model animal systems, which will ultimately provide a methodology applicable to examining human sputum samples. To develop the necessary analytical flow techniques for quantitative assessment of cellular damage, cell analysis and sorting instrumentation developed at the Los Alamos Scientific Laboratory (4) is currently being used to characterize initially respiratory tract cells from the Syrian hamster which has been selected as the experimental test system.

The approach is to adapt cell preparation and staining techniques previously developed (5) and to characterize respiratory cells using the multi-parameter cell analysis (6) and multiangle light-scatter (7) systems. This includes the acquisition of exfoliated respiratory cells by lavaging the lungs with saline; adaptation of cytological techniques designed for dispersing human gynecological specimens to hamster lung epithelium for obtaining single-cell suspensions; utilization of existing staining techniques for measurement of cellular biochemical parameters; and initial characterization using flow instrumentation. Examples of preliminary results from studies involving characterization of respiratory tract cells based on nonspecific esterase activity, two-color acridine orange fluorescence, RNA content, protein, cell size, nuclear and cytoplasmic diameter, and multiangle light-scatter properties are presented in this report. As the flow technology is adapted further to

analyze respiratory tract cells, measurement of early changes in the various cellular properties as a function of exposure to toxic materials will be performed.

#### MATERIALS AND METHODS

##### Sample Acquisition, Preparation, and Staining

Normal Syrian hamsters were sacrificed by administering 15 mg of sodium pentobarbital intraperitoneally. The trachea was surgically exposed, intubated with a 19-gauge, 3.5-cm blunt-tipped, stainless steel needle bent 45° at the midpoint and attached to a syringe containing 3 ml of physiological saline, and then was secured around the needle by tying with chromic gut. The respiratory tract posterior to the larynx was then sequentially lavaged (3,4) four times to obtain exfoliated cells. Differential counts, summarized in Table 1, indicate that samples were composed primarily of macrophages, leukocytes, ciliated columnar cells, and basal undifferentiated cells plus small debris. Clumps and sheets of epithelial cells were disaggregated by forcing (syringing) the suspension through a 25-gauge needle.

To demonstrate nonspecific esterase activity in respiratory tract cells and subsequent viability, unfixed samples (2.5 ml) were stained with fluorescein diacetate (FDA, 10  $\mu$ l of 0.5 g FDA/100 ml acetone) at 0° for 30 min using the "fluorochromasia" procedure (9) and analyzed for total fluorescence. Live cells accumulate fluorescein intracellularly when FDA is hydrolyzed by esterases, since the free fluorescein cannot pass out through the intact cell membrane. Unfixed samples were also stained with acridine orange (AO, 100  $\mu$ l of 10  $\mu$ g AO/ml saline) at room temperature and analyzed for two-color nuclear (green) and cytoplasmic (red) fluorescence.

Samples fixed in 35% ethanol were stained for DNA using mithramycin (10, 11) and analyzed for total DNA content and cell size by measuring fluorescence and small-angle light scatter, respectively. Fixed samples were also stained for DNA and protein using propidium iodide (PI) and fluorescein isothiocyanate (FITC), respectively (11,12), and analyzed for two-color red and green fluorescence properties. Nuclear and cytoplasmic diameters were determined from analog signal time durations as described below. Samples stained with FDA, AO, and mithramycin remained in the stain solution during analysis, whereas PI-FITC stained cells were rinsed and resuspended in saline for two-color fluorescence analysis.

#### Instrumentation

The principle of measurement was as follows (Fig. 1). Cells stained in liquid suspension flowed through a chamber ( $10^3/\text{sec}$ ) at a nearly constant velocity and intersected a narrow, elliptically shaped, argon laser beam. As cells crossed the narrow wall of laser illumination, bound dyes were excited to fluoresce and cells scattered light, the laser wavelength settings being 457 and 488 nm for excitation of mithramycin and FDA/AO/PI-FITC, respectively. Both fluorescence and light scatter were electro-optically measured, the fluorescence sensors being dual photomultiplier tubes which quantitated total or two-color fluorescence of selectable color separation regions. Light scatter was measured by optically focusing the forward light scattered at  $0.7$  to  $2.0^\circ$  onto a photodiode detector (13).

Nuclear and cytoplasmic diameters were determined by electronically measuring the time required for the cell nucleus and cytoplasm to pass across the "thin wall" of laser illumination. For example, as mithramycin-stained cells

crossed the laser beam, analog fluorescence (nucleus) and light-scatter (cytoplasm) were converted electronically into signals, the

amplitude of which was proportional to the respective diameter (14). Nuclear and cytoplasmic diameter measurements were determined similarly from PI-FITC stained cells by measuring the red (nucleus) and green (cytoplasm) fluorescence signal time durations (15). Both methods are similar in concept to the "slit-scan" principle previously described by Wleceless (16,17).

Optical signals proportional to the various cellular parameters were processed as single parameters or two-parameter combinations. A multichannel pulse-height analyzer accumulated and displayed signals as pulse-amplitude frequency distribution histograms (Fig. 1). After optical measurement, cells emerged from the flow chamber exit nozzle in a stream (liquid jet) which was broken into uniform droplets, thus isolating cells into droplets with approximately 2% containing a single cell (18). When experiments required cells to be separated, processed signals corresponding to the specific region of a distribution in which cells to be separated were located activated an electronic time delay which then triggered a droplet charging pulse. This caused a group of droplets containing the cell of interest to be charged and deflected by a static electric field into a collection vessel. Sorted cells were then introduced into a cytocentrifuge and deposited onto a microscope slide for counterstaining and identification.

In addition to measuring small-angle light scatter, a flow instrument capable of measuring light scatter at 32 angles simultaneously (7) has been used to analyze respiratory tract cells. As cells pass through the flow chamber and intersect a helium-neon laser beam, scattered light is detected using a circular photodiode array, measured values stored in a computer, and then processed to form a scatter diagram of light-scatter intensity vs angle. The scatter data are then converted into a cluster diagram which permits individual light-scatter patterns from each cell to be grouped according to a mathematical clustering algorithm (19).

## RESULTS

Figure 2 shows a typical fluorescence distribution recorded on a hamster lung washing after treatment with FDA. The distribution has three distinct regions of cells composed of peaks 1, 2, and 3. Respiratory tract cells corresponding to peaks 2 (channels 20-60) and 3 (channels 60-95) have been identified by sorting and microscopic examination as being made up principally of leukocytes and macrophages, respectively. Cells corresponding to the much smaller peak 1 have not been identified positively but are under further investigation. Similar data from other hamsters indicate that the total number of cells within the different regions varies from animal-to-animal (3). Further tests are also planned to determine where basal undifferentiated and ciliated columnar cells are located in the distributions and to determine if FDA activity is correlated with cell volume.

Our initial results have demonstrated that respiratory tract cells can be characterized using a two-color AO fluorescence method similar to that previously described for differentiating human blood peripheral leukocytes (20) in which the nucleus fluoresces green and the cytoplasm (granules) red. The green and red fluorescence distribution recorded on a cell sample stained with AO is shown in Fig. 3. The green fluorescence distribution is nearly unimodal, illustrating somewhat uniform nuclear staining, and is also similar to that obtained for human leukocytes. However, the gated red fluorescence distribution, which reflects primarily cytoplasmic granulation, shows three distinct regions. Peaks 1, 2, and 3 have not yet been identified by the cell separation methods described above, but experiments are under way to determine the cells contained within these regions.

Results obtained from measurement of DNA content, cell size, and nuclear and cytoplasmic diameter are illustrated in Fig. 4. Figure 4A shows the DNA



distribution in which the first peak represents cells having 2C diploid DNA content and the second peak doublets and binucleated cells having 4C DNA content (3). The cell size distribution (small-angle light scatter), which was obtained by recording only those light-scatter signals coincident with fluorescence signals (DNA content), is broad, indicating a wide range of cell sizes composed primarily of two major regions (peaks 1 and 2) as illustrated in Fig. 4B.

The nuclear diameter distribution (Fig. 4C), which was obtained from fluorescence signal time duration measurements, is essentially unimodal, indicating cells with nuclei similar in size. Peak 2 of Fig. 4C represents a small portion of the population composed of cell doublets and those which are binucleated. The gated cytoplasmic diameter distribution (Fig. 4D), determined from small-angle light-scatter signal time duration measurements in coincidence with fluorescence signals, indicates a minimum of two cell types.

Similar data recorded on other respiratory tract washings show a minimum of three cell types. Experiments are currently in progress to verify what cells correspond to the different peaks in the respective diameter distributions and to improve the resolution of diameter measurements.

Two-color fluorescence analysis of DNA content, total protein, and nuclear and cytoplasmic diameter in respiratory tract cells stained with PI-FITC is shown in Fig. 5. The DNA content distribution (Fig. 5A) is unimodal but somewhat broader than that recorded earlier using the mithramycin technique (Fig. 4A). This increased broadness is thought to be due, in part, to spectral color overlap that exists between PI and FITC. The gated protein distribution (Fig. 5B), which was obtained by recording only those green (protein) signals coincident with red (DNA) fluorescence signals, is broad and indicates a wide range in

cellular protein content. The nuclear diameter distribution (Fig. 5C), which was obtained from red fluorescence signal time duration measurements, is unimodal and similar to that recorded using mithramycin (Fig. 4C). However, the gated cytoplasmic diameter distribution (Fig. 5D), derived from green fluorescence signal time durations coincident with DNA content signals, is bimodal and shows a minimum of two cell populations differing in diameter by about 2.0. Future experiments will involve separating cells based on cytoplasmic diameter measurements for identification purposes.

In studies designed to measure subtle differences in cell morphology, flow multiangle light-scatter techniques have been used to analyze exfoliated hamster respiratory tract cells based on differences in scatter patterns (Fig. 6). At least three groups can be distinguished based on the angular light-scatter intensity measurements (2). Recent data indicate that possibly four to five cell types may be detected using this methodology. Future experiments will involve separating cells differing in their light-scatter patterns and identifying what types correspond to the regions of the cluster diagram. Such are dependent upon the addition of cell sorting capability to the multi-angle light-scatter flow system (7) which is presently under way.

#### DISCUSSION

These results demonstrate the potential capability of applying multi-parameter flow-systems technology to analyze exfoliated respiratory tract cells, the ultimate goal being development of cytological and biochemical indicators for use in estimating damage to lung epithelium of humans exposed by inhalation to toxic agents. Respiratory tract cells from normal hamsters will continue to be analyzed using the different flow-analysis methods for the required initial characterizations. These will include DNA content, protein,

cell size, enzyme activity, nuclear and cytoplasmic size relationships including nuclear-to-cytoplasmic ratios, and multiangle light-scatter properties. Cells will be characterized more extensively based on these parameters and, in addition, will be separated and morphologically identified. As experimentation proceeds, it may be necessary also to modify the cell preparation and staining procedures and instrumental analysis methods developed in the initial studies. In addition, continued emphasis will be placed on new methods which may be potential indicators of atypical cellular changes. As the flow technology becomes adapted to the analysis of respiratory tract cells, measurement of physical and biochemical cellular properties as a function of exposure to toxic agents will be performed on groups of experimental and control animals, with the results ultimately being extrapolated to humans.

#### ACKNOWLEDGMENTS

This work was performed under the auspices of the U. S. Energy Research and Development Administration, with joint support from the U. S. Environmental Protection Agency (agreement EPA-IAG-D5-E681). We thank M. Ingram, R. G. Thomas, and D. M. Smith (consultations); J. Grilly (photography); and E. M. Sullivan (manuscript preparation).

## REFERENCES

1. J. A. Steinkamp, M. Ingrassia, K. M. Hansen, and J. S. Wilson, Detection of Early Changes in Lung Cell Cytology by Flow-Systems Analysis Techniques. Los Alamos Scientific Laboratory report LA-0267-PP (Mar. 3, 1976).
2. J. A. Steinkamp, K. M. Hansen, J. S. Wilson, and G. C. Salzman, Detection of Early Changes in Lung Cell Cytology by Flow-Systems Analysis Techniques. Los Alamos Scientific Laboratory report LA-0267-PP (August 1976).
3. J. A. Steinkamp, K. M. Hansen, J. S. Wilson, and G. C. Salzman, Detection of Early Changes in Lung Cell Cytology by Flow-Systems Analysis Techniques. Los Alamos Scientific Laboratory report LA-0267-PP (December 1976).
4. P. F. Mullaney, J. A. Steinkamp, H. A. Crissman, L. S. Cram, and P. M. Holtz, Laser flow microphotometers for rapid analysis and sorting of individual mammalian cells. In: Laser Applications in Medicine and Biology, Vol. 2 (M. L. Wolbarst, ed.), Plenum Press, New York-London (1974), p. 151.
5. H. A. Crissman, P. F. Mullaney, and J. A. Steinkamp, Methods and applications of flow systems for analysis and sorting of mammalian cells. In: Methods in Cell Biology, Vol. 10 (D. M. Prescott, ed.), Academic Press, New York (1975), p. 1079.
6. J. A. Steinkamp, M. J. Fulwiler, J. R. Coulter, K. D. Hiebert, J. L. Horney, and P. F. Mullaney, A new multiparameter separator for microscopic particles and biological cells. Rev. Sci. Instrum. 44, 1301 (1973).
7. G. C. Salzman, J. M. Crowell, C. A. Goad, K. M. Hansen, K. D. Hiebert, P. M. LaBauve, J. C. Martin, and P. F. Mullaney, A flow-system multiangle

- light-scattering instrument for cell characterization. Clin. Chem. 21, 1297 (1975).
8. H. Schreiber and P. Nettesheim, A new method for pulmonary cytology in rats and hamsters. Cancer Res. 32, 737 (1972).
  9. B. Rotman and B. W. Papermaster, Membrane properties of living mammalian cells as studied by enzymatic hydrolysis of fluorogenic esters. Proc. Natl. Acad. Sci. USA 55, 134 (1966).
  10. H. A. Crissman and R. A. Tobey, Cell cycle analysis in twenty minutes. Science 184, 1297 (1974).
  11. H. A. Crissman, M. S. Oka, and J. A. Steinkamp, Rapid staining methods for analysis of DNA and protein in mammalian cells. J. Histochem. Cytochem. 24, 64 (1976).
  12. H. A. Crissman and J. A. Steinkamp, Rapid, simultaneous measurement of DNA, protein, and cell volume in single cells from large mammalian cell populations. J. Cell Biol. 59, 766 (1973).
  13. P. F. Mullaney, M. A. Van Dilla, J. R. Coulter, and P. N. Dean, Cell sizing: A light scattering photometer for rapid volume determination. Rev. Sci. Instrum. 40, 1029 (1969).
  14. J. A. Steinkamp, K. M. Hansen, and H. A. Crissman, Flow microfluorometric and light scatter measurement of nuclear and cytoplasmic size in mammalian cells. J. Histochem. Cytochem. 24, 291 (1976).
  15. J. A. Steinkamp and H. A. Crissman, Automated analysis of DNA, protein, and nuclear to cytoplasmic relationships in tumor cells and gynecologic specimens. J. Histochem. Cytochem. 22, 616 (1974).
  16. L. L. Wheelless and S. F. Patten, Slit-scan cytofluorometry. Acta Cytol. 17, 333 (1974).

17. L. L. Wheeless, J. A. Hardy, and J. Balasubramanian, Slit-scan flow system for automated cytopathology. *Acta Cytol.* 19, 45 (1975).
18. M. J. Fulwyer, Electronic separation of biological cells by volume. *Science* 150, 910 (1965).
19. C. A. Goad, A MUMPS Code-Building Package for Data-Base Management. Los Alamos Scientific Laboratory report LA-6065-MS (September 1975).
20. L. R. Adams and L. A. Kamentsky, Machine characterization of human leukocytes by acridine orange fluorescence. *Acta Cytol.* 5, 289 (1971).

TABLE 1. Differential cell counts of normal hamster respiratory tract cell samples obtained by lavaging the lungs with normal saline<sup>a</sup>

Hamster Number	Macrophages (%)	Leukocytes (%)	Basal Undifferentiated Cells (%)	Ciliated Columnar Cells (%)
1	74	18	7	1
2	79	14	6	1
3	74	17	7	2
4	44	43	12	1

<sup>a</sup>Determined microscopically from Papanicolaou-stained samples.

**Fig. 1.** Diagram of the multiparameter cell separator system, illustrating laser excitation, flow chamber, fluorescence and light-scatter sensors, signal processing, and cell separation electronics, and droplet charging and deflection scheme.



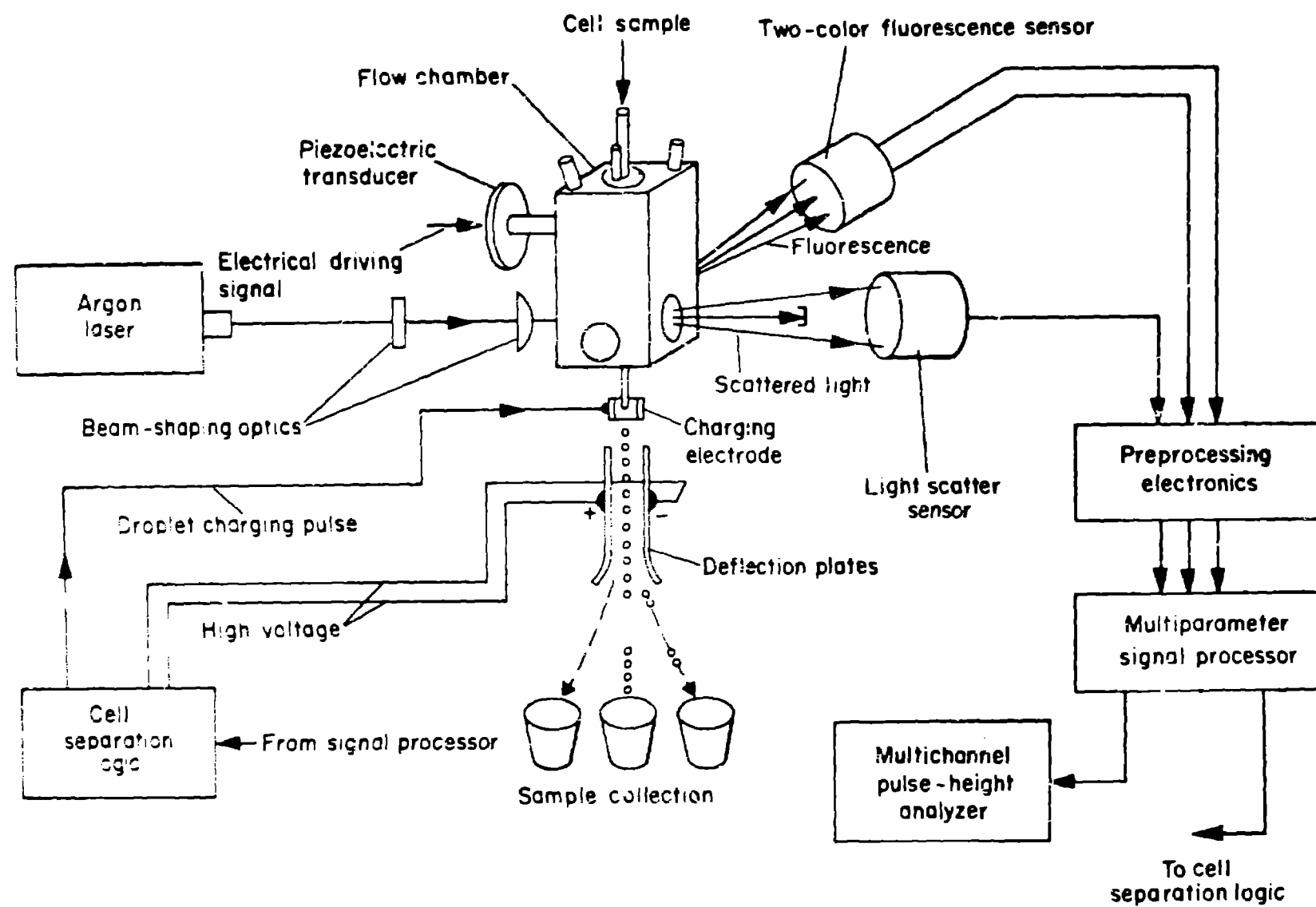


**Fig. 2.** Frequency distribution histogram of a normal hamster respiratory tract washing stained with fluorescein diacetate (FDA) and analyzed for fluorescence. The horizontal axis is proportional to the logarithm of intracellular fluorescence (three decades). Cells corresponding to peaks 2 and 3 have been identified as leukocytes and macrophages, respectively. Peak 1 is under investigation.

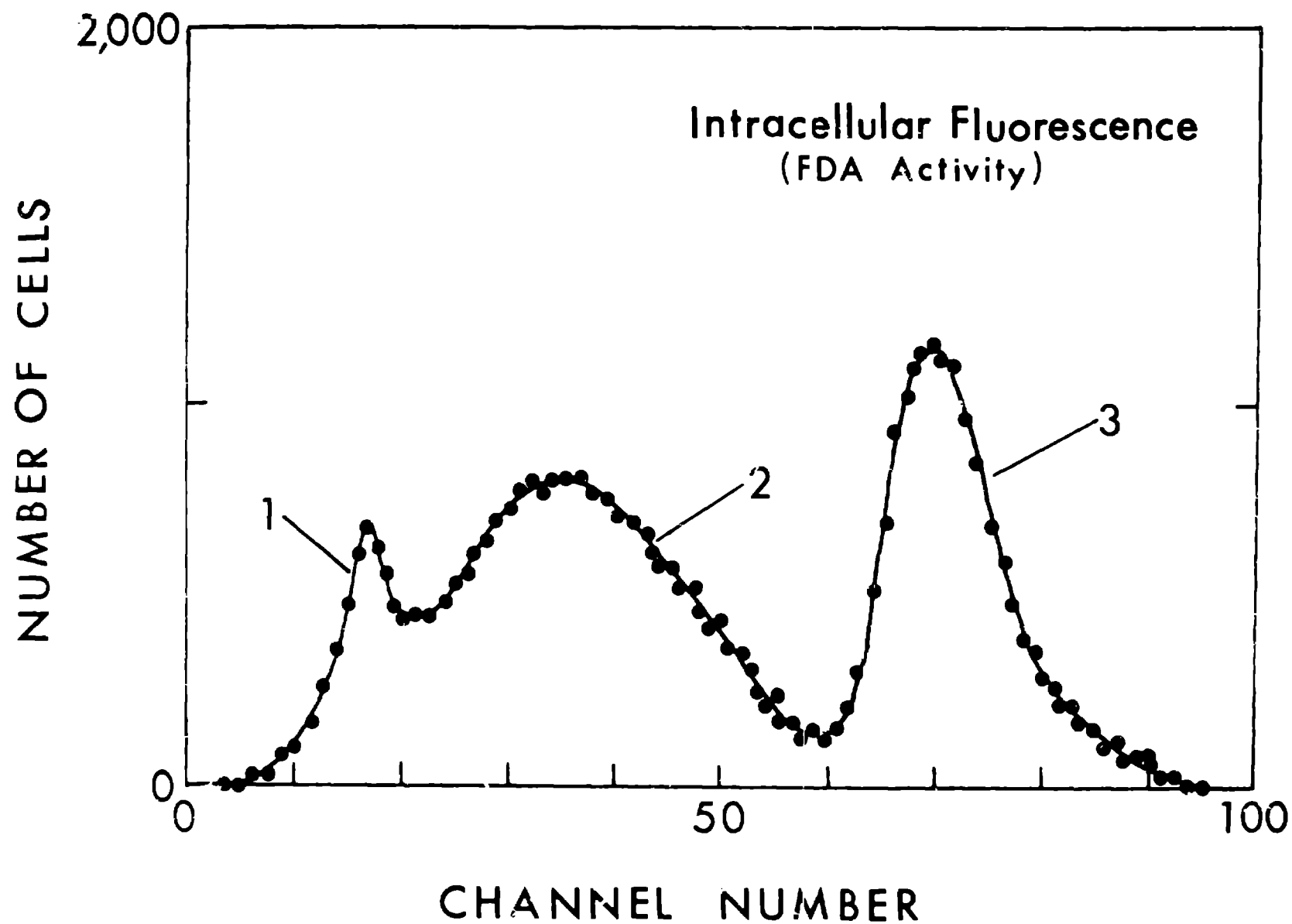


**Fig. 3.** Frequency distribution histograms of a normal hamster respiratory tract washing stained with acridine orange (AO) and analyzed for two-color fluorescence: (A) green nuclear fluorescence and (B) gated red cytoplasmic fluorescence obtained by recording only red fluorescence signals coincident with green nuclear fluorescence. The horizontal axes of both distributions are proportional to the logarithm of fluorescence signal amplitude (three decades). Cells corresponding to peaks 1, 2, and 3 of (B) have not been identified but are under investigation.

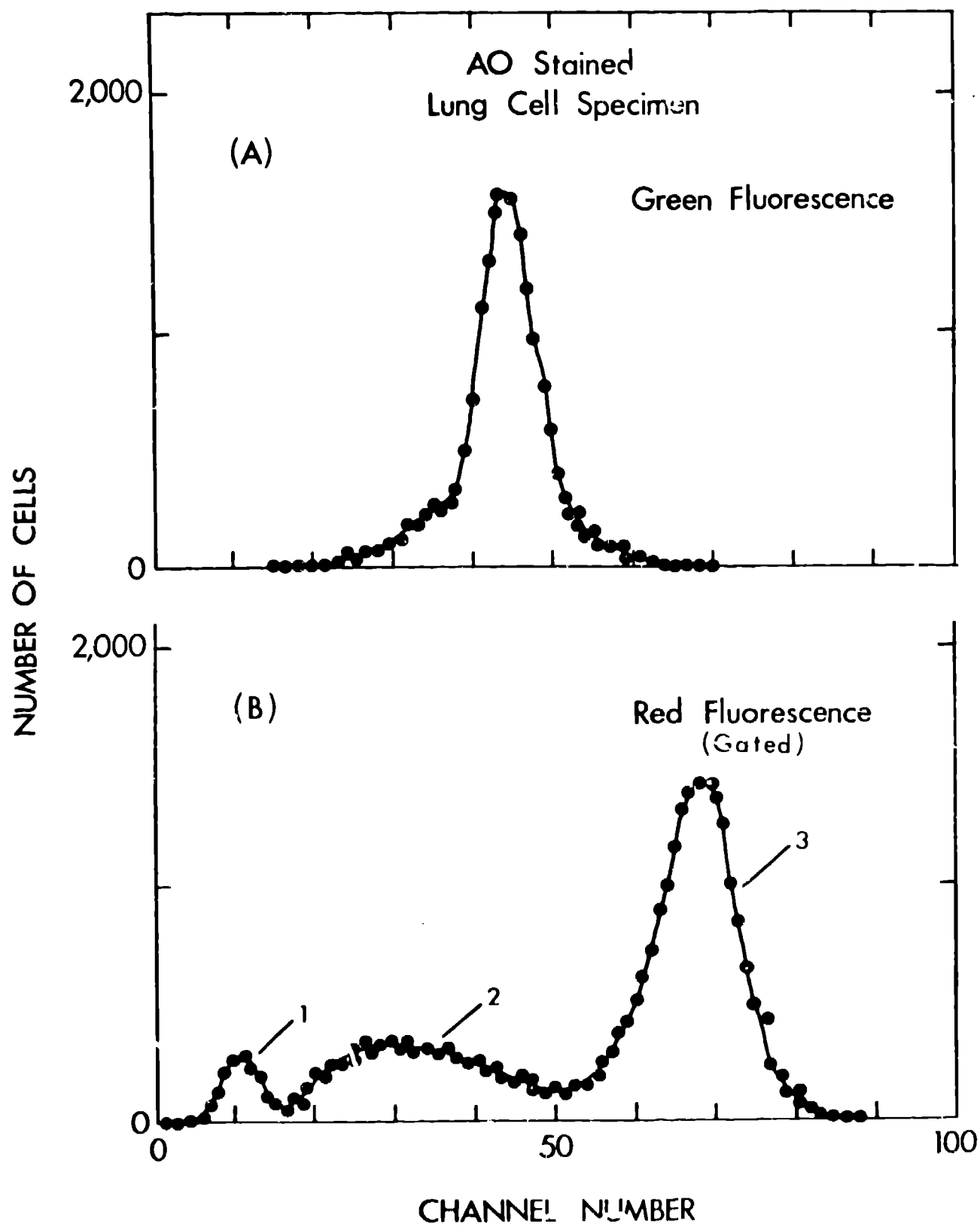


Fig. 4. Frequency distribution histograms of DNA content, cell size, and nuclear and cytoplasmic diameter for a normal hamster respiratory tract washing fixed and stained with mithramycin and analyzed for fluorescence and light-scatter properties: (A) DNA content; (B) cell size of nucleated cells obtained by recording only light-scatter signals from fluorescing cells; (C) nuclear diameter obtained from fluorescence signal time durations; and (D) cytoplasmic diameter obtained by recording only light-scatter signal time durations from fluorescing cells. Peaks 1 and 2 of (A) and (C) represent cells having 2C diploid DNA content and 4C DNA content (doublets and binucleated cells), respectively. Peaks 1 and 2 of (B) and (D) represent nucleated cells and have not been positively identified.

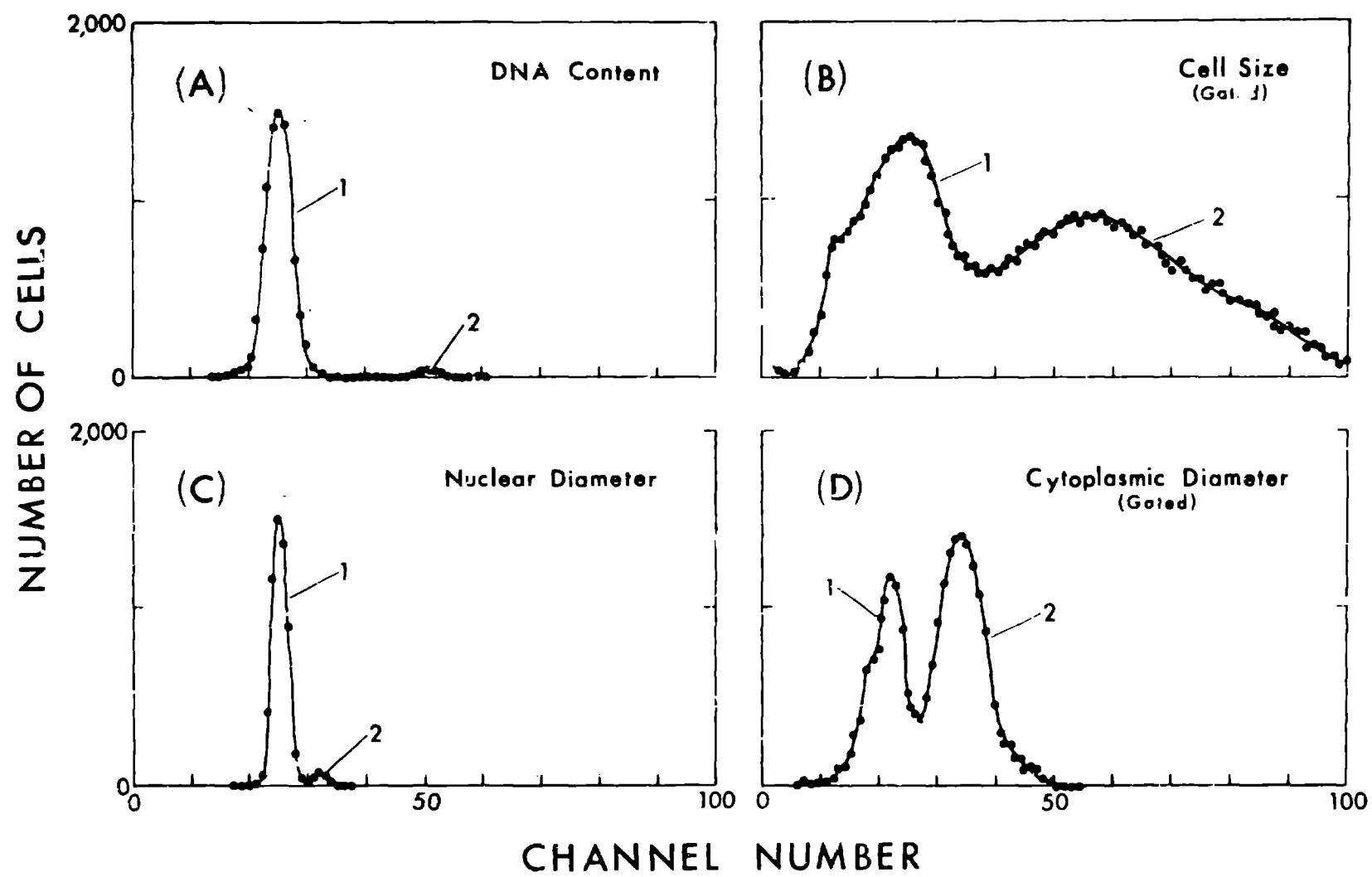


Fig. 5. Frequency distribution histograms of DNA content, total protein, and nuclear and cytoplasmic diameters from a normal hamster respiratory tract washing fixed and stained with PI-FITC and analyzed for two-color fluorescence properties: (A) DNA content; (B) total protein obtained by recording only green fluorescence signals from nucleated cells; (C) nuclear diameter obtained from red nuclear fluorescence signal time durations; and (D) cytoplasmic diameter obtained by recording only green fluorescence signal time durations from nucleated cells. Cells corresponding to peaks 1 and 2 of (B) and (D) have not been positively identified and are under investigation.



NUMBER OF CELLS

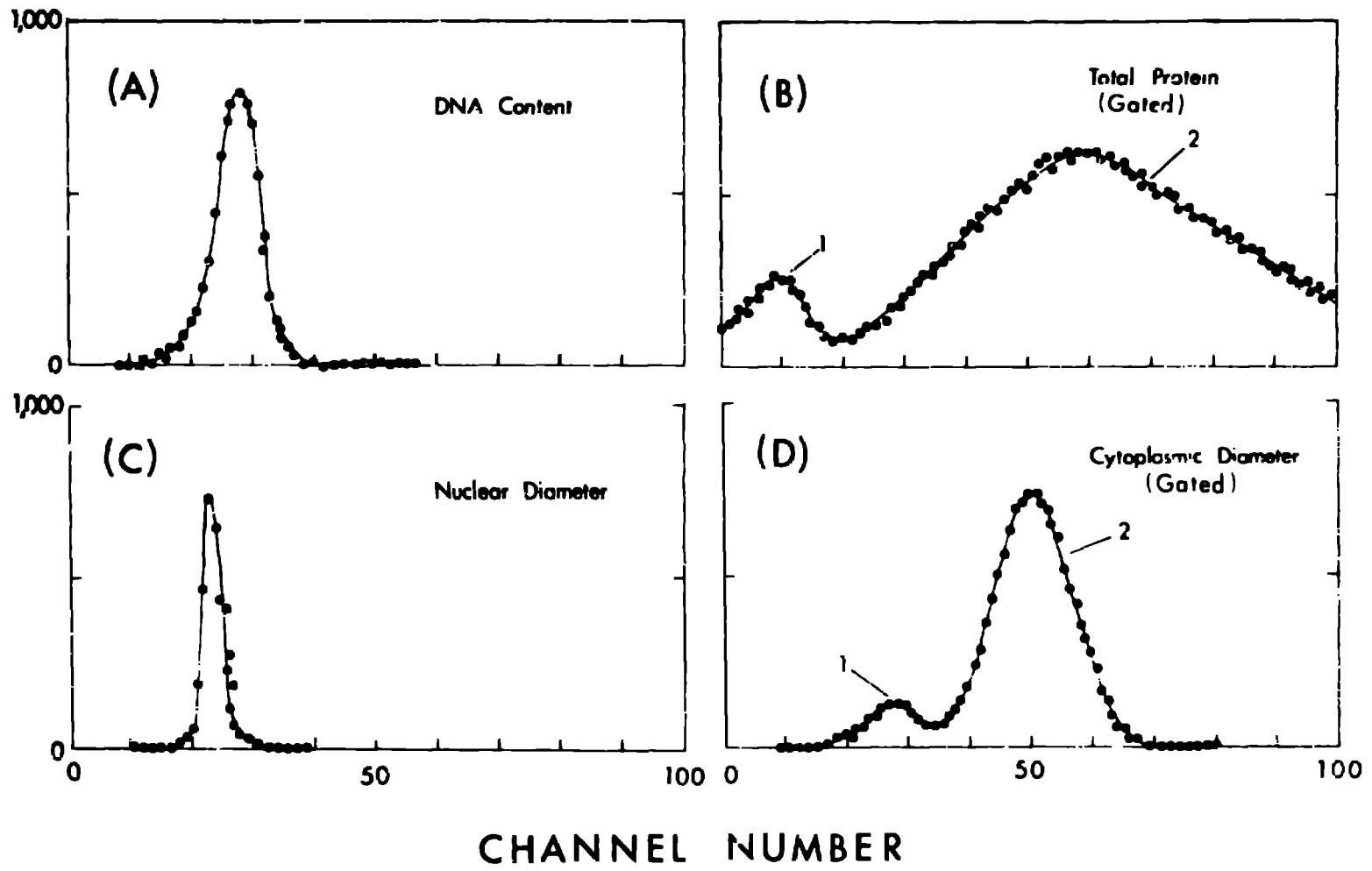


Fig. 6. Cluster diagram derived from multiangle light-scatter pattern (three decade log intensity vs angle) recorded on a normal hamster respiratory tract cell sample. Each cluster, which represents a cell size grouping, is enclosed by a broken or solid line and shows an excursion of one standard deviation from the mean. The percentages represent the approximate number in each size class (cluster). Cells corresponding to the clusters have not been positively identified and are under investigation.

